ISSN 0020-1685, Inorganic Materials, 2024. © Pleiades Publishing, Ltd., 2024.

On the Reasons for the Premature Failure of Safety Valve Springs in the Equipment of Primary Oil Refining

M. A. Tupitsin[a], *, I. A. Trishkina[a], and E. I. Storozheva[a]

[a] *Research, Design, and Technological Institute of Oil Refining and Petrochemical Equipment, Volgograd, 400078 Russia*

**e-mail: matupicin@vnikti.rosneft.ru*

Received November 22, 2022; revised December 16, 2022; accepted February 28, 2023

Abstract—The reasons for the premature failure of a spring (made of 50KhFA steel) used in the safety valve of the column head part are analyzed. The failure of the spring occurred after 7 years of operation at a temperature below 90°C in a working environment of light oil products (sulfurous gasoline). Visual and measurement control, general chemical analysis of the composition of the steel, energy-dispersive analysis of the metal in local areas, measurements of hardness and microhardness, microstructural analysis of the metal, macro- and electron fractography, phase chemical and X-ray structural analyses, and recovering heat treatment are used for the studies. The characteristic external signs, typical microdamages, and mechanisms of sulfide (hydrogen) corrosion cracking of high-strength 50KhFA steel with the most dangerous accompanying process, hydrogenation, are revealed. The analysis of the chemical composition and hardness of the metal meets the requirements of the standards for this steel. The microstructure of the metal under study is tempered martensite with the presence of a decarburized layer of up to 0.158 mm in the surface layers. The results of the study show that the premature failure of the spring is attributed both to the technological heredity and operational factors (contact with the working environment beyond the design basis). Ulcerative damage of the metal surface with the penetration of corrosion products into the deep layers due to the violation of the integrity of the coating of the spring are noted, which indicates low resistance of 50KhFA steel to low-temperature hydrogen sulfide corrosion. The failure predominantly occurs near nonmetallic inclusions along the boundaries of the primary austenite grains, where the largest precipitates of chromium carbides are located, as well as along the interphase boundaries of oriented carbide plates.

Keywords: 50KhFA steel, spring, safety valve, failure, fracture, low-temperature hydrogen sulfide corrosion, cracking, mechanism of failure

DOI: 10.1134/S0020168524700213

INTRODUCTION

Uninterrupted operation of the equipment in the oil refining industry depends on the reliability of safety valves, the most important part of which is springs.

The durability and reliability of springs are foreseen at the stage of design and should be provided both by the manufacturing procedure and quality control and operational conditions [1, 2]. The diagnostics of the state of the safety valve and springs is performed in the process of operation in the manner and to the extent provided for by the actual regulatory documents, e.g., IPKM-05 "Procedure for the Operation, Revision, and Repair of Safety Valve Springs and Membrane Safety Devices of Oil Refining and Petrochemical Enterprises of the Ministry of Industry and Energy of Russia."

However, cases of premature failure of springs are noted during the operation of safety valves at oil refineries. The aspects of damageability of safety valve springs during the operation of oil refining units are covered in the published sources to a lesser extent in comparison with the aspects of damageability of equipment and pipelines. In addition, published sources mainly describe the results of fractographic studies of metals [3–10]. Here, there is almost no information on the application of other methods of laboratory examination of failed springs which are equally informative. Therefore, the development of a procedure of laboratory examination of safety valve springs for determining the causes for premature failure as well as recommendations on their safe operation for oil refining systems is of certain scientific interest and has practical significance.

OBJECT AND METHOD OF STUDY

The object of study was an SPPK 4-150-16M safety valve spring installed at the outlet from a column into the flare system of one of the crude oil distillation units. The spring failed after 7 years of operation at a design lifetime of at least 30 years and mean time before failure of 360 cycles. The operating temperature of the valve was below 90°C, and the operating environment of the pipeline was light oil products (sulfu-

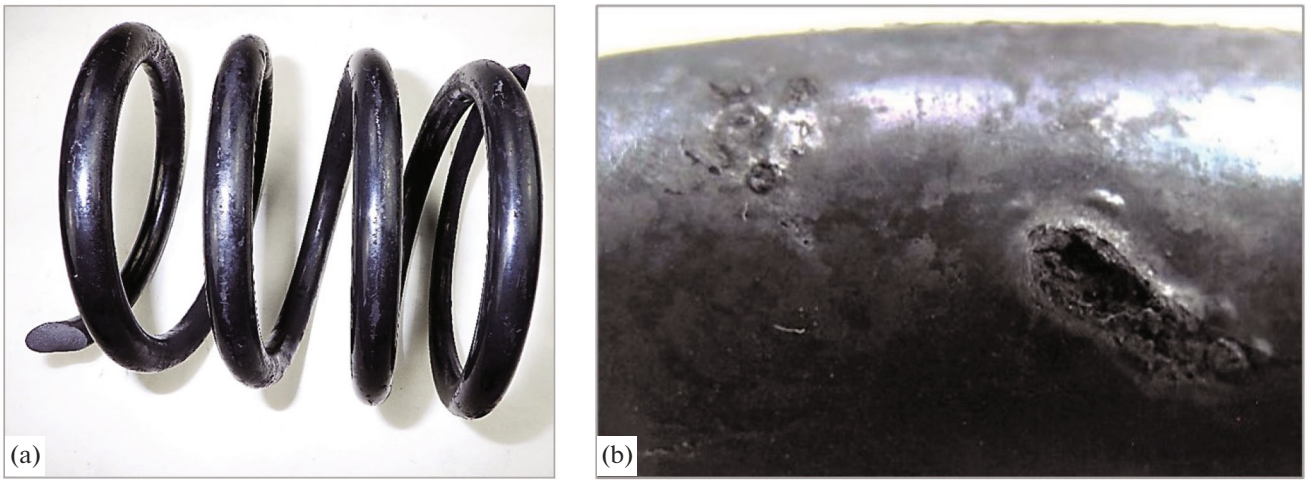

Fig. 1. Fragments of the spring after failure: (a) general view and (b) defects on the turns.

rous gasoline). The material of the cylindrical spiral compression spring of the studied safety valve was 50KhFA steel that is characterized by high operational properties such as limit of elasticity, limit of endurance, and relaxation resistance.

To establish the reasons for the failure of the spring, classical methods of investigation and state-of-the-art instruments as well as modeling of the initial structural and mechanical state of the material of the spring before operation by recovering heat treatment were applied. Visual and measurement control, general chemical analysis of the composition of the steel, energy-dispersive analysis of the metal in local areas, measurement of hardness for the determination of the quality of heat treatment, microstructural analysis of the metal, macro- and electron fractography, phase chemical and X-ray diffraction analyses, measurement of microhardness, and recovering heat treatment according to the mode recommended for safety valve springs in ST TsKBA 030-2006 regulatory technical documentation and published sources [11], namely, quenching at 860 ± 10°C and medium-temperature tempering at 420 ± 10°C, were performed during the study.

For metallographic studies, a hardware–software complex for the analysis of the surface microstructure of solid bodies based on an optical microscope as well as a scanning electron microscope with the identification of the structural components, investigation of their morphology and mutual orientation, and determination of the presence of modified structures in the surface layers and defects was used. The chemical composition of the steel was determined and carbide analysis of the metal was performed by analytical methods with the use of a spectrophotometer, an automated titrator, and a rapid carbon analyzer. The X-ray diffraction analysis was performed on an X-ray apparatus. The microhardness was measured on a microhardness meter with a load of 100 g. In addition, the precipitates collected from the surface of the spring were studied by energy-dispersive analysis.

RESULTS AND DISCUSSION

The appearance of a fragment of the spring with the surface of a fracture is presented in Fig. 1a. The visual and measurement control showed the correspondence of the number of turns, external diameter of the spring, diameter of the rod, and other dimensions to the initial parameters of the spring according to the manufacturer's specification. There was a protective paint-and-varnish coating with exfoliation, blistering, and peeling on the surface of the spring; lateral wear, corrosion deposits, and corrosion spots were seen. Cracks and voids were located in the areas of corrosion spots and blisters (Fig. 1b). The defects detected upon external examination of the springs are considered unallowable in accordance with i. 6.7.3 of IPKM-2005 Instruction.

The chemical composition of the material of the spring (Table 1) corresponded to 50KhFA steel according to GOST (State Standard) 14959-2016.

The hardness of the steel measured on microsections before and after recovering heat treatment (Table 2) conformed to the requirements of ST TsKBA 030-2006 and data of reference literature. The values of hardness indicated a high-quality heat treatment performed by the manufacturer.

No defects specified by GOST 14959-2016 were detected in the macrostructure of the material.

Contamination was determined by method Sh according to GOST 1778-70—the nonmetallic inclusions corresponded to spot oxides (second rating) and sulfides (first rating).

A zone of decarburization was observed on the surface of the spring turns (along the entire perimeter of circumference) (Fig. 2a). The decarburized layer had a depth of 0.114 to 0.158 mm (the error of measure-

Table 1. Results of the analysis of the chemical composition of the steel

Material	Weight part of elements, %							
	C	Si	Mn	Cr	V	Ni	S	P
Spring	0.56 ± 0.04*	0.30	0.475	0.93	0.200	0.120	0.012	0.026 ± 0.006*
50KhFA Steel (V 14959–2016)	0.46–0.54 ± 0.01**	0.17–0.37	0.50–0.80	0.80–1.10	0.10–1.20	≤0.25	≤0.025	≤0.025

* Error of the method of determination of the element.
** Allowable deviation of the concentration of the element according to the standard.

Table 2. Results of the measurement of the hardness of the steel

Material	Hardness HRC
Spring under study, initial state in the transverse cross section	46–47 (47)
Spring under study, initial state in the longitudinal cross section	44–47 (45)
Spring under study after recovering heat treatment in the transverse cross section	45–46 (46)
50KhFA steel (ST TsKBA 030-2006)	44.0–51.5
50KhFA [11]	44–49

The average values are indicated in brackets.

ment of ±1 μm). According to GOST 14959-2016, the presence of a decarburized layer is not allowed for hot-rolled rods with a special surface finish, while for other types of rolled products, the depth of the decarburized layer should not exceed a value of 0.015*d*, where *d* is the nominal diameter of the rod (in this case, 14 mm), i.e., 0.21 mm. The decarburized layer could have formed during process of operations upon the fabrication of the spring. No decarburized layer was detected on the surface of the heat-treated section (Fig. 2b) as a result of diffusion redistribution of carbon over the cross section.

The microstructure of the metal after operation and recovering heat treatment (Figs. 3, 4) is tempered martensite. The observed shape of carbides in the form of plates that are characteristic of spring steel after quenching and medium-temperature tempering as opposed to coagulated carbides after high-temperature tempering indicates high elastic properties of the spring.

The results of phase X-ray diffraction analysis of the spring (Table 3) indicate that the main type of carbides in the metal under study is special carbide Me_7C_3 + MeC, in particular, $(Cr,Fe)_7C_3$ + VC typical of 50KhFA steel in the state after medium-temperature tempering and operation at 90°C.

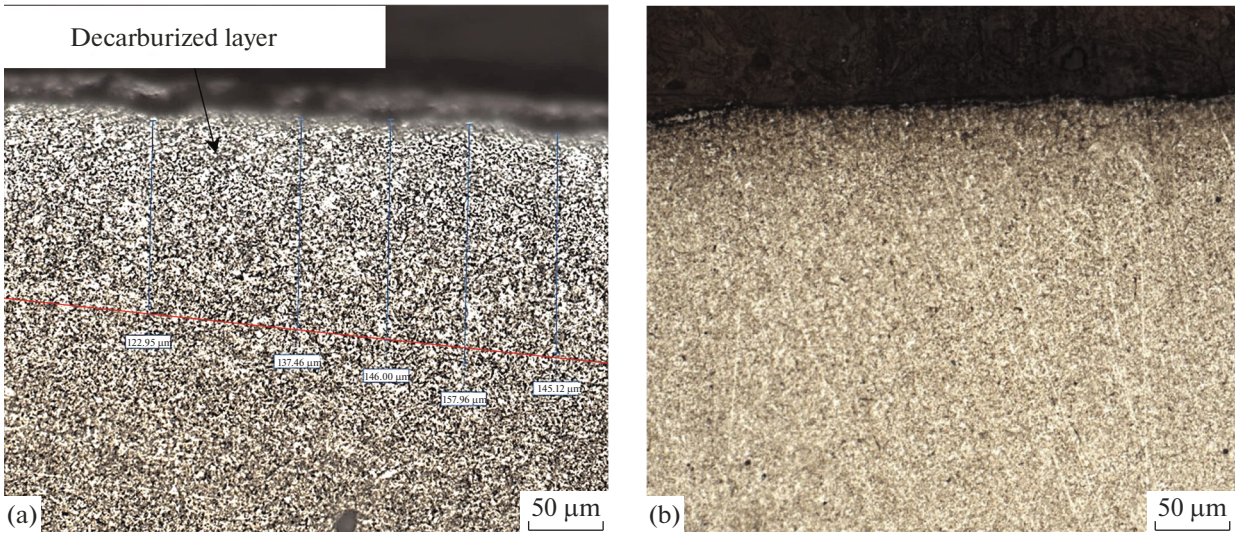

Fig. 2. Surface of the metal section (a) before and (b) after heat treatment, ×200.

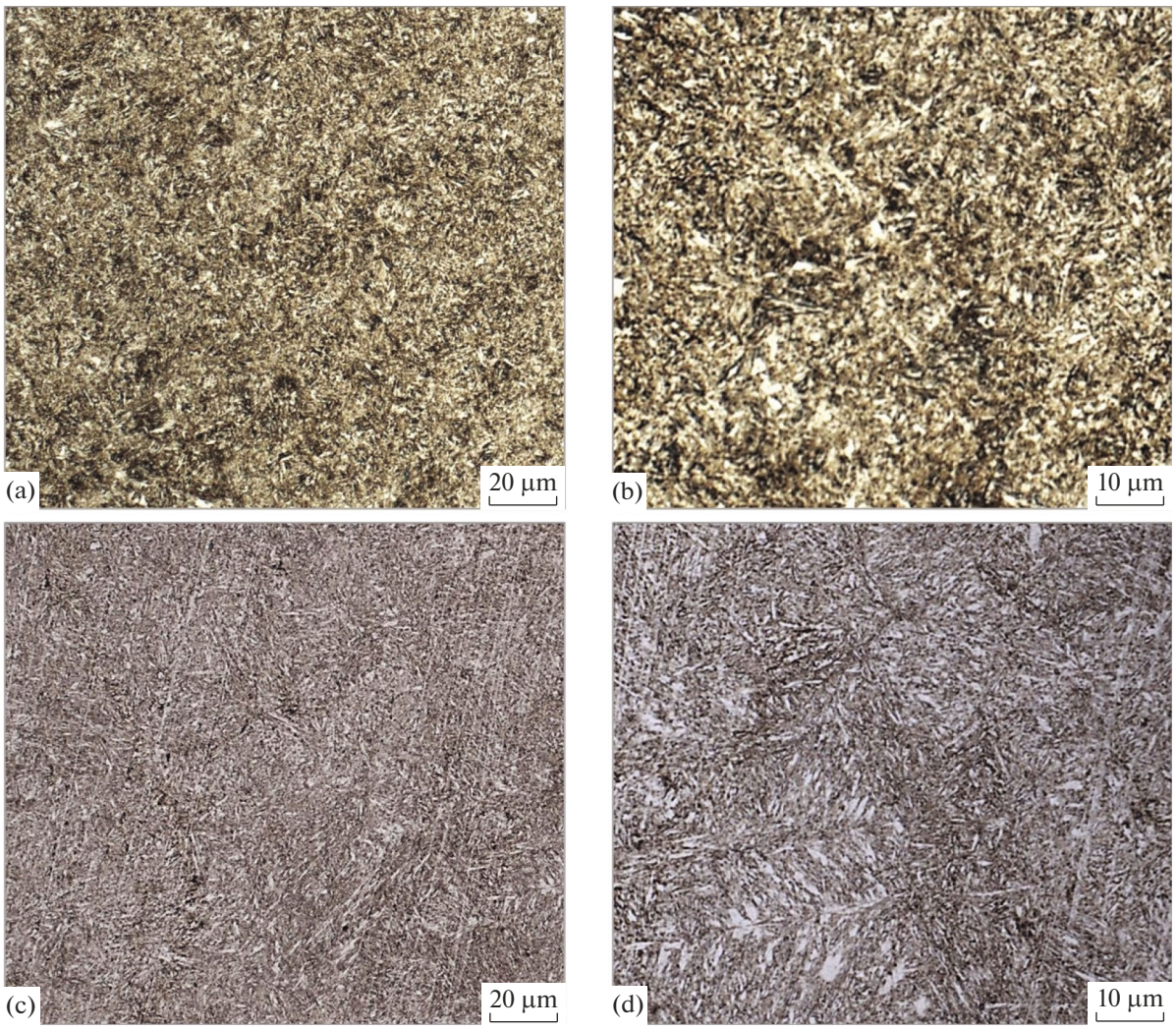

Fig. 3. Initial microstructure of the microsection of the steel (a, b) before and (c, d) after heat treatment: (a, c) ×500 and (b, d) ×1000.

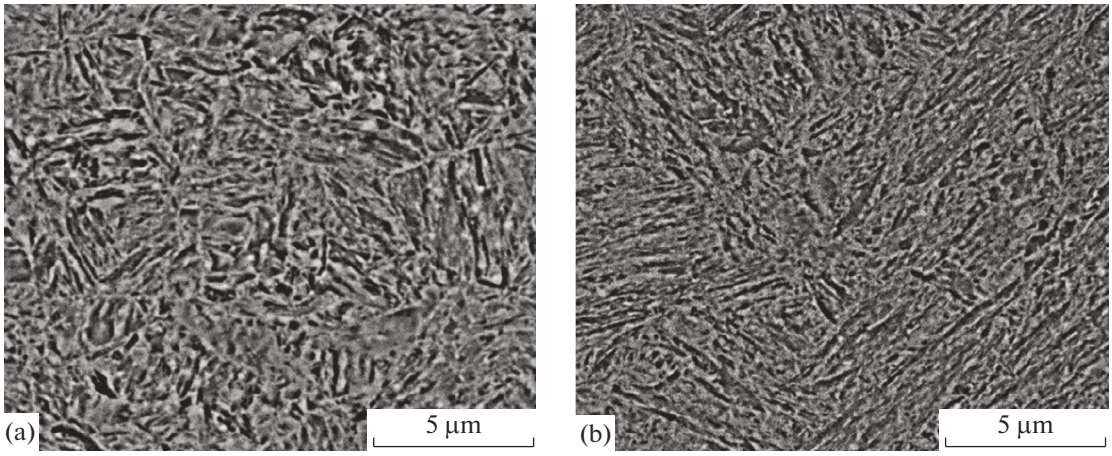

Fig. 4. Morphology of the carbide phase in the steel, ×10000 (SEM image): (a) after operation and (b) after recovering heat treatment (operation + quenching + tempering).

Table 3. Results of carbide analysis

Material	Concentration of elements, wt %						Relative concentration of the element in carbides, %		Type of carbides
	carbide precipitate				solid solution				
	Fe	Cr	V	Σ	Cr	V	Cr	V	
50KhFA	1.43	0.126	0.148	1.704	0.804	0.052	13	74	Me_7C_3 + VC

Table 4. Microhardness $HV_{0.1}$ of the metal measured on a microsection

Edges of the microsection	Central part of the microsection	Decarburized layer of the microsection
570–570 (570)	570–570 (570)	351–351 (351)

The average values are indicated in brackets.

The phase chemical analysis has shown that only 13% chromium transformed into carbides, while the remaining part stayed in a solid solution and provides a solid-solution strengthening mechanism in addition to carbide and dislocation mechanisms. However, the total chromium content cannot provide corrosion resistance in the working environment of the safety valve under consideration. Protection against the working environment getting onto the surface of the spring by both high-quality sealing of the demountable connections of the valve and protective coating that turned out to be damaged is required.

The minimum values of the microhardness of the metal measured over the cross section of the rod corresponded to the zone of the decarburized layer (Table 4). Since most elastic elements operate under the conditions of twisting when the maximum stresses fall within the surface layer in particular, the presence of a soft decarburized layer promoted the damage of the surface under the paint-and-varnish coating and origination of a fracture nucleus.

The study of the microstructure near the fracture nucleus has shown the presence of multiple surface defects in the form of pitting corrosion, cracks, splitting over the nonmetallic inclusions, and corrosion products penetrating into the deep layers of the metal (Fig. 5, Table 5). Microcracks originated from corrosion ulcers in the sites of damage of the protective coating and predominantly propagated along the grain boundaries to form closed contours and cavities filled with corrosion products, from which new microcracks developed. The analysis of the chemical elements in the microcracks and cavities indicates a significant concentration of sulfur and oxygen, which points to the occurrence of hydrogen sulfide corrosion.

Figure 5 shows the damage over the elements of the structure and morphology of the cracks on the sections after etching with a 4% solution of HNO_3. The cracks propagate not only along the boundaries of the primary austenite grains, where the largest precipitates of carbides are located, but also along the interphase boundaries of the oriented plates of carbides. There

Table 5. Chemical composition of the scanned areas in Figs. 5e and 5f

Element	Fig. 5e		Fig. 5f	
	at %	wt %	at %	wt %
Fe	38.15	61.34	60.44	76.66
O	37.42	17.24	34.01	17.66
S	18.90	17.45	4.22	4.39
C	2.79	0.96	0.53	0.21
Si	1.28	1.03	–	–
Cr	0.84	1.26	–	–
Ca	0.62	0.71	0.35	0.32

are also pores in the solid solution matrix (Fig. 6). The tiniest micropores with a size of up to 0.5 μm in martensite (Fig. 6b) have also been detected on the sections cut out far from the surface of the spring, which may be associated with the presence of hydrogen in steel which is formed in the case of occurrence of low-temperature hydrogen sulfide corrosion.

It has been found by the fractographic study that the fracture is matt, dark gray. The fracture surface is oriented at an angle of 45° to the axis of the rod and is perpendicular to the direction of action of the maximum stretching stresses upon twisting; there is a concavity in the central part which is characteristic for quasi-brittle materials [15]. The macrogeometry of the fracture indicated the formation of fracture in the process of operating loads. In terms of the macrostructure, the fracture of the spring was characterized by the following successive zones: 1—fracture nucleus zone with a smooth relief, 2—scarring zone that corresponds to the development of a crack, and 3—fast fracture zone with less rough areas (Fig. 7). A loss of the protective coating and ulcerous damage of the surface were observed near the nucleus determined by the convergence of the scars and located on the outer surface of the spring between the small and large radii of the turn (see Fig. 7). The small size of the nucleus zone

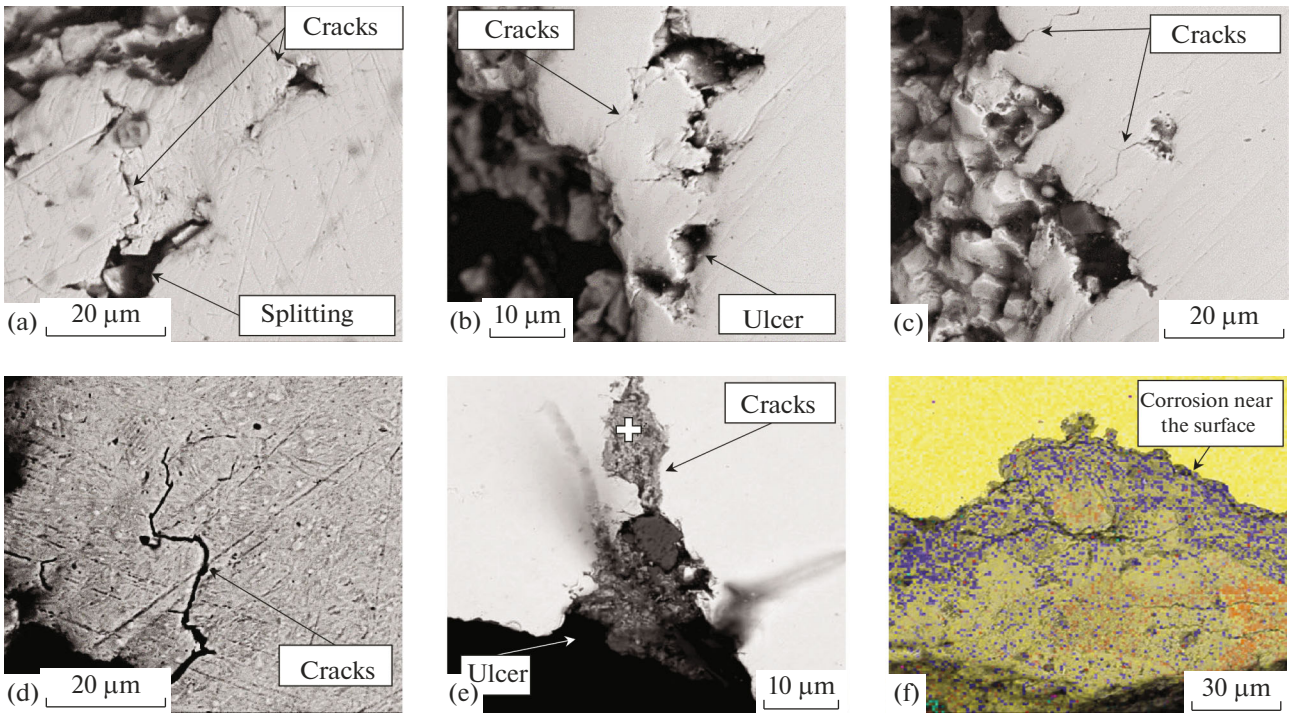

Fig. 5. Defects of the metal of the spring at the fracture nucleus: (a–c) pitting corrosion, microcracks, and cavities (prior to etching); (d) cracks along the grain boundaries of primary austenite (after etching); (e, f) composition of corrosion products in the cracks.

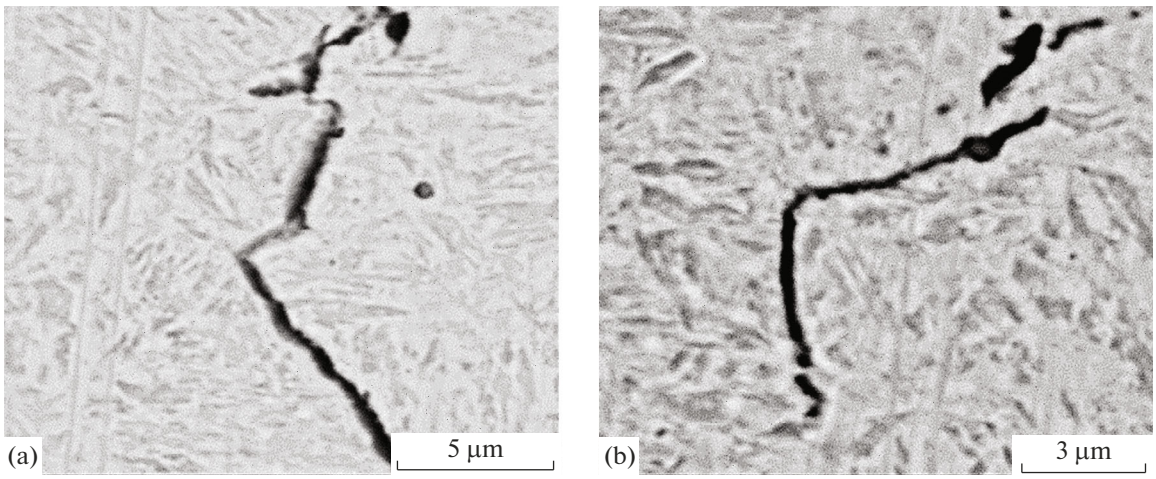

Fig. 6. Appearance of the cracks after etching: (a) ×15000 and (b) ×20000.

and a low number of circular lines corresponding to the front of crack propagation indicated high stresses.

According to the electron fractographic studies, corrosion products are present in the fracture nucleus that coincides with the site of damage of the coating, while individual areas with fatigue striations are present in the decarburized surface layer; there are also opened bubble cavities, bubbles with cracks (Figs. 8a, 8g), nonmetallic inclusions, and intergrain facets and cracks characteristic of hydrogen sulfide corrosion cracking (Figs. 8b, 8h). In the failure development zone (Figs. 8c, 8d, 8i), cleavage and quasi-cleavage facets, splitting along nonmetallic inclusions, and pores typical of decelerated failure under the action of hydrogen can be seen [4, 12, 14–16]. The fracture surface in the scarring zone is formed by intercrystalline failure facets with alternation of a quasi-cleavage and individual areas of pit relief. The fast fracture is also char-

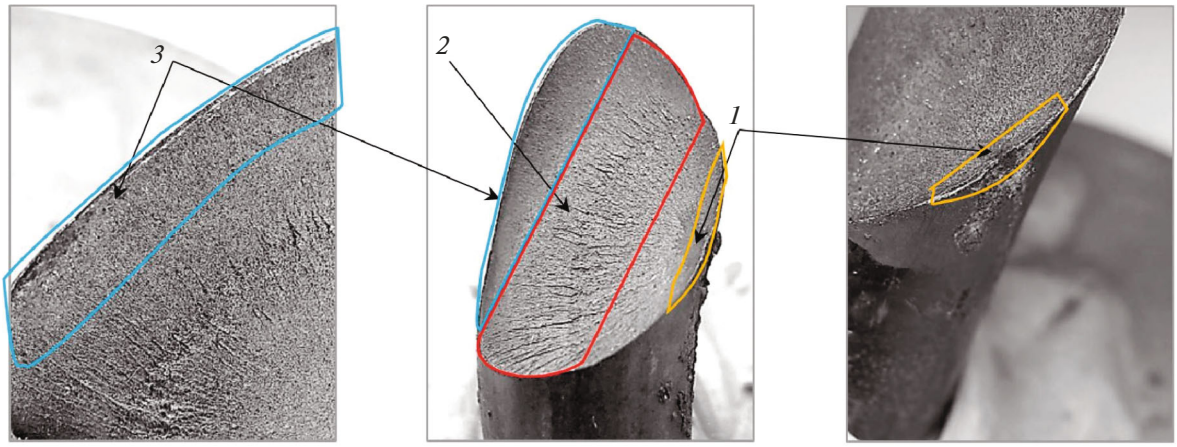

Fig. 7. General view of the fracture of the spring: (*1*) fracture nucleus, (*2*) crack propagation zone, and (*3*) fast fracture zone.

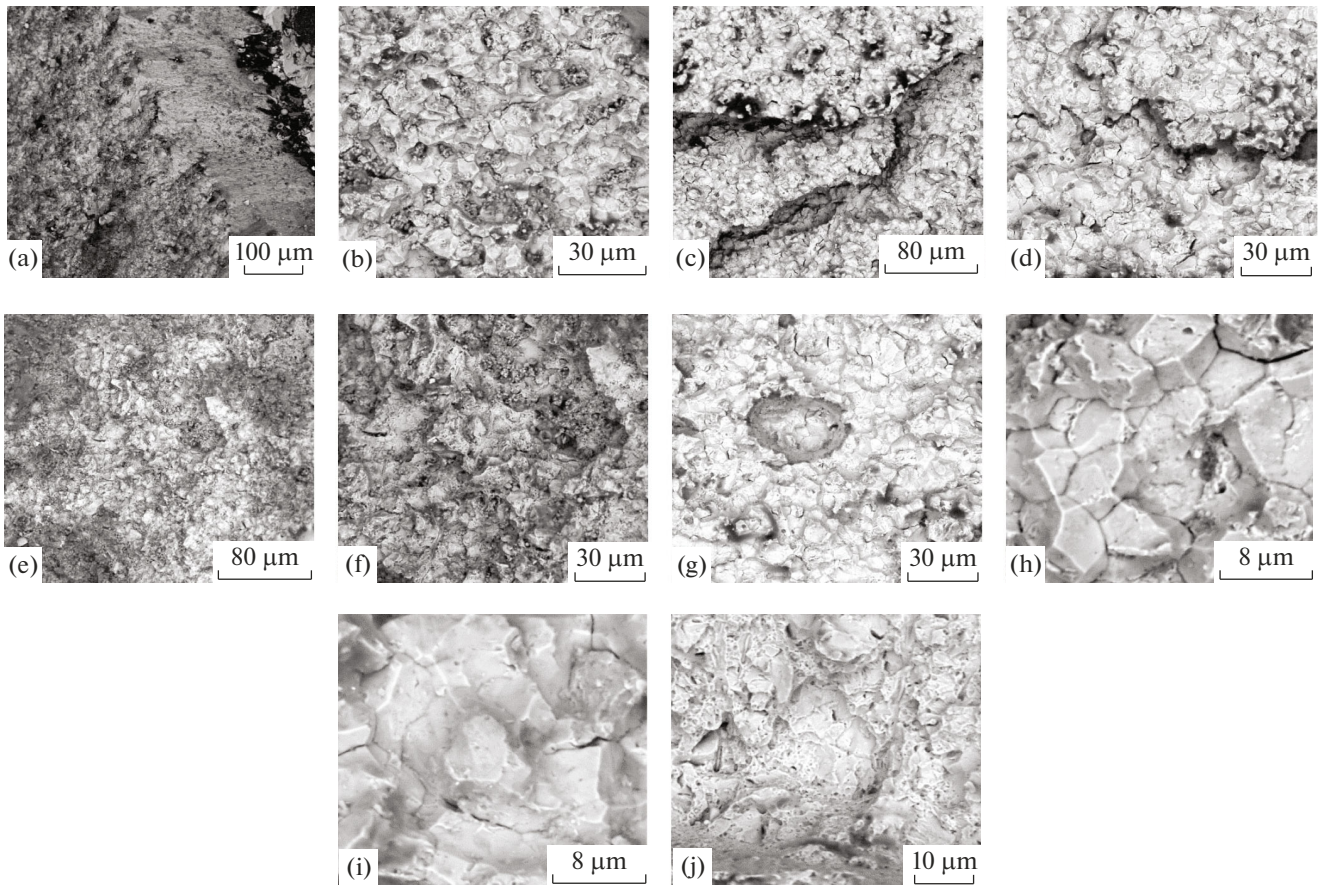

Fig. 8. Electron fractograms of the fracture surface of the spring: (a, b) fracture nucleus; (c, d) fracture development, scarring zone; (e, f) fast fracture; (g) bubbles; (h, i) intergrain facets, cleavage facets, quasi-cleavage facets, splitting, multiple cracks, pores; and (j) splitting by sulfides, pits.

acterized by facets of intercrystallite and transcrystallite failure with areas of pit relief (Figs. 8e, 8f, 8j).

The deposits collected from the surface of the spring have been studied by energy-dispersive analysis (Fig. 9). The presence of iron and oxygen in the deposits indicates that the corrosion products consist of iron oxides; the presence of sulfur suggests sulfur-containing compounds—iron sulfides formed by the

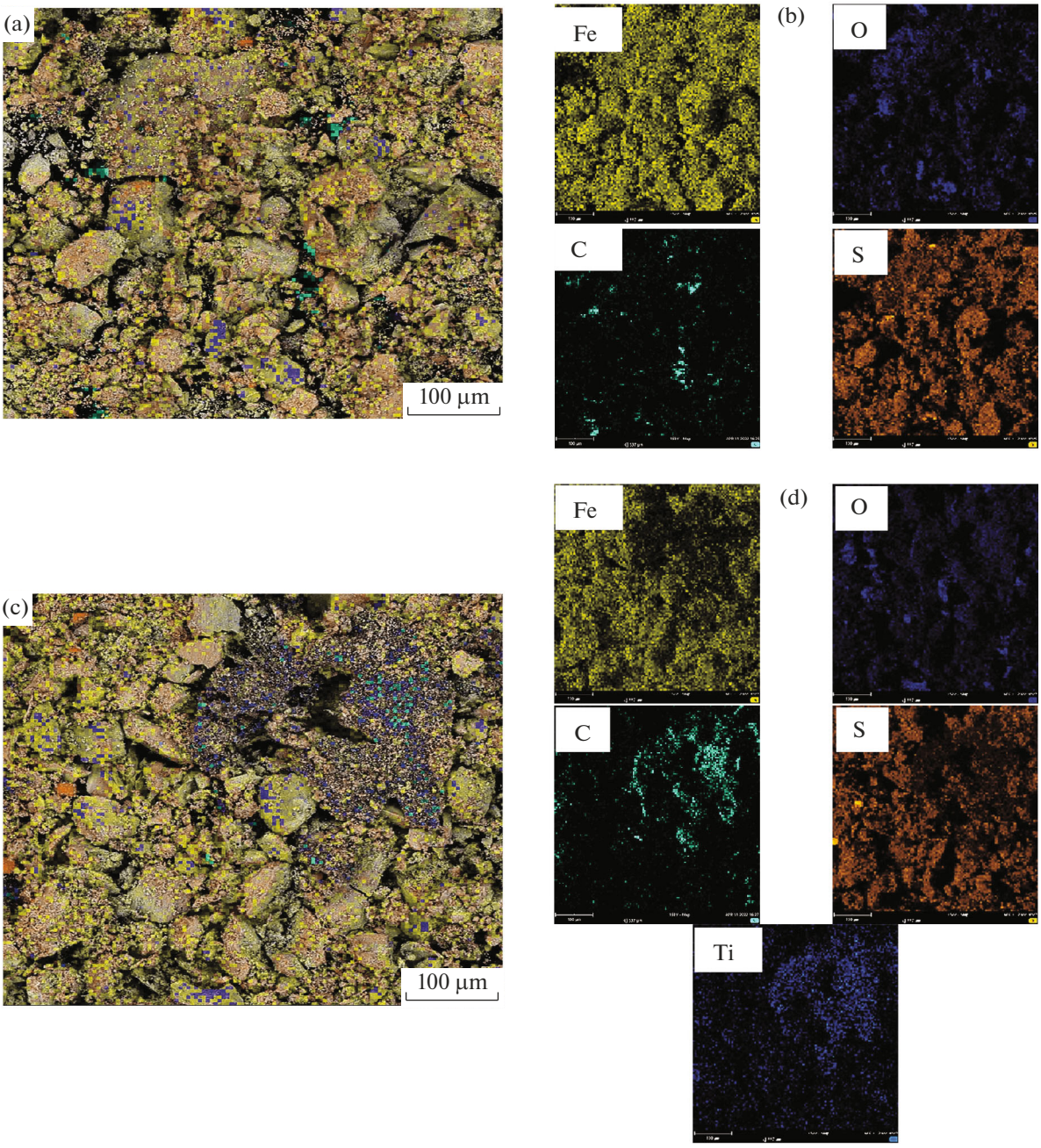

Fig. 9. (a, c) Results of the analysis of the deposits on the metal surface and (b, d) data of energy-dispersive analysis.

action of the hydrogen sulfide present in the environment. Titanium found in a small amount could be present in the composition of the pigment of the protective paint-and-varnish coating.

The combination of the obtained results of the study made it possible to draw a conclusion that the reason for the failure of the spring was sulfide (hydrogen) corrosion cracking of high-strength steel. The most dangerous accompanying process of low-temperature hydrogen sulfide corrosion is hydrogenation of steel, which is confirmed by the presence of blisters under the deposits. Such blisters result from the presence of hydrogen sulfide itself or hydrogen evolving during the reaction of hydrogen sulfide with iron under the deposits. Hydrogen, diffusing deep into the steel, is accumulated in the sites of presence of crystal lattice defects and nonmetallic inclusions, and over time it forms internal pores and induces the develop-

ment of microcracks that eventually result in the creation of significant internal stresses and embrittlement of the metal. The presence of moisture in the environment significantly accelerates low-temperature hydrogen sulfide corrosion and hydrogenation of steel, thus accelerating its embrittlement.

CONCLUSIONS

(1) It has been found that, in the case of low-temperature hydrogen sulfide corrosion of 50KhFA steel, blisters and ulcerous damage with the penetration of corrosion products into the deep layers are formed on the surface of the spring. Failure of the metal near the nonmetallic inclusions and cracking along the boundaries of the primary austenite grains, where the largest precipitates of chromium carbide are located, as well as along the interphase boundaries of the oriented plates of carbides, occur. When the cracks form an almost closed contour, the metal deforms under the pressure of hydrogen, followed by the formation of cavities that decrease the resistance to operating loads and result in failure. Micropores with a size of up to 0.5 μm which are not healed by recovering heat treatment have been detected in the solid solution.

(2) The results of the analysis of the deposits have shown the presence of sulfur compounds in the corrosion products on the surface of the spring, which may indicate that it is affected by hydrogen sulfide present in the vapors of the gasoline leaving the column.

(3) The premature failure of the safety valve spring is determined by the technological heredity (system of doping which does not provide corrosion resistance in the environment of hydrogen sulfide, formation of a soft and weak decarburized layer under the paint-and-varnish coating which decreases the limit of endurance during the fabrication of the spring, insufficient protection of the spring against corrosion by the paint-and-varnish coating) upon contact with a working environment not specified by the design.

(4) On the basis of the studies performed, a set of actions to increase the reliability and to prevent failures of the springs of SPPK valves operating under similar conditions has been recommended: execution of periodic visual and measurement control and magnetic particle inspection or liquid penetrant testing; observation of the state of the sealing surfaces; need for replacing the spring in the case of discovery of the described damage of the paint-and-varnish coating; provision of high quality of the assembly of the valve after repair and coaxial alignment of positioning of the part; and application of protective covers—bellows made of steel of 08Kh18N10T type or more corrosion-resistant steels for similar springs which do not allow penetration of aggressive agents to the surface of the spring. The acquired information on the characteristic external signs, typical microdamage, and failure mechanism upon low-temperature hydrogen sulfide corrosion of 50KhFA steel with the most dangerous accompanying process, hydrogenation, can be used by researchers in the diagnostics of failures of springs.

FUNDING

This work was supported by ongoing institutional funding. No additional grants to carry out or direct this particular research were obtained.

CONFLICT OF INTEREST

The authors of this work declare that they have no conflicts of interest.

REFERENCES

1. Makaryants, G.M., Fatigue failure mechanisms of a pressure relief valve, *J. Loss Prevent. Process Ind.,* 2017, vol. 48, pp. 1–13. https://doi.org/10.1016/j.jlp.2017.03.025
2. Kumar, T.S.M. and Adaveesh, B., Application of '8D methodology' for the root cause analysis and reduction of valve spring rejection in a valve spring manufacturing company: A case study, *Indian J. Sci. Technol.,* 2017, vol. 10, no. 11, pp. 1–11. https://doi.org/10.17485/ijst/2017/v10i11/106137
3. Goritskiy, V.M., Analysis of the reasons for the destruction of safety valve springs, *Khim. Neft. Mashinostr.,* 1994, no. 4, pp. 27–29.
4. Goritskiy, V.M., *Diagnostika metallov* (Metal Diagnostics), Moscow: Metallurgizdat, 2004.
5. Engel, L., *Rastrovaya elektronnaya mikroskopiya. Razrushenie* (Scanning Electron Microscopy. Destruction), Moscow: Metallurgiya, 1986.
6. Grigorenko, V.B., The use of fractographic analysis to determine the causes of destruction of products from medium carbon steels, *Tr. VIAM,* 2018, no. 8, pp. 98–111.
7. Liu Bo-Chao and Yang Zhan-Guo, Failure analysis of shock absorption spring is motorcycle, *J. Fail. Anal. Prevent.,* 2016, no. 16, pp. 337–345. https://doi.org/10.1007/s11668-016-0112-3
8. Das, S., Taukdar, S., Solanki, V., Kumar, A., and Mukhopadhyay, G., Breakege of spring steel during manufacturing: A metallurgical investigation, *J. Fail. Anal. Prevent.,* 2020, no. 20, pp. 2462–1469. https://doi.org/10.1007/s11668-020-00993-9
9. Xing, X.Q. et al., Effect of environment-assisted cracking on the premature fatigue failure of high-strength valve springs, *Eng. Fail. Anal.,* 2021, vol. 126, pp. 105466. https://doi.org/10.1016/j.engfailanal.2021.105466
10. Pal, U., Mukhopadhyay, G., and Bhattacharya, S., Failure analysis of spring of hydraulic operated valve, *Eng. Fail. Anal.,* 2019, vol. 95, pp. 191–198. https://doi.org/10.1016/j.engfailanal.2018.09.013

11. Sorokin, B.G., Volosnikova, A.V., and Vyatkin, S.A., *Marochnik stalei i splavov* (Grader of Steel and Alloys), Moscow: Mashinostroenie, 1989.

12. Tupitsin, M.A. et al., Study of the influence of structural heritage and operating conditions on the durability of safety valve springs from steel 50KHFA, *Mater. Phys. Mech.,* 2022, vol. 48, no. 2, pp. 161–174. https://doi.org/10.18720/MPM.4848(2)2022

13. Goldshtein, M.I. et al., *Spetsial'nye stali* (Special Steels), 2nd ed., Moscow: MISIS, 1999.

14. Houdremont, E.A., *Handbuch der Sonderstahlkunde,* Berlin: Springer, 1943, vol. 2.

15. Fellose, J., *Fractography and Atlas of Fractographs,* Vol. 9 of *Metals Handbook,* 8th ed., Materials Park, OH: Am. Soc. Metals, 1974.

16. Ren, C.X. et al., Enhanced bending fatigue resistance of a 50CrMnMoVNb spring steel with decarburized layer by surface spinning strengthening, *Int. J. Fatig.,* 2019, vol. 124, pp. 277–287. https://doi.org/10.1016/j.ijfatigue.2019.03.014

17. Grigorenko, V.B. and Morozova, L.V., Peculiarities of destruction of hardware made of steel 30KhGSA, *Zavod. Lab. Diagn. Mater.,* 2018, vol. 84, no. 5, pp. 45–54. https://doi.org/10.26896/1028-6861-2018-84-5-45-54

Translated by E. Boltukhina